

# Optimized resonant capacitor and switching frequency for high-efficiency wireless power transfer in E-bikes using CST Studio Suite

Wan Muhamad Hakimi Wan Bunyamin, Rahimi Baharom

Power Electronics Research Group, Faculty of Electrical Engineering, Universiti Teknologi MARA, Selangor, Malaysia

## Article Info

### Article history:

Received Aug 13, 2025

Revised Dec 8, 2025

Accepted Jan 9, 2026

### Keywords:

Efficiency optimization

Electric vehicle

Resonant technique

Switching frequency

Wireless power transfer

## ABSTRACT

Wireless power transfer (WPT) is increasingly adopted for E-bike charging; however, its performance is often constrained by inaccurate resonant tuning, inefficient capacitor selection, and improper switching-frequency operation, which lead to significant power loss and reduced transfer efficiency. This study addresses these limitations by formulating an optimized design methodology for selecting resonant capacitors and inverter switching frequency to achieve high-efficiency energy transfer. A 40-mm air gap between the transmitter and receiver coils is modeled using CST Studio Suite, where a 3D electromagnetic circuit co-simulation framework is applied to evaluate mutual inductance, resonant behavior, magnetic-field distribution, and S-parameter characteristics. Parametric sweeps combined with a convergence-based optimization algorithm identify the optimal resonant operating point, yielding a peak resonant frequency of 38.1 kHz, a maximum simulated transfer efficiency of 99%, and a deep reflection coefficient of -21.77 dB. The optimized configuration also demonstrates stable voltage and field distribution at resonance, confirming effective impedance matching. The main contributions of this work include: i) establishing a unified EM-circuit optimization workflow for determining resonant capacitance and switching frequency, ii) providing quantitative resonance parameters and performance indicators suitable for compact E-bike WPT systems, and iii) integrating mathematical modelling to validate CST-based predictions and ensure theoretical consistency. The proposed approach significantly enhances design accuracy and efficiency, offering a scalable and high-performance solution for next-generation low-power electric vehicle (EV) and E-bike wireless charging applications.

This is an open access article under the [CC BY-SA](https://creativecommons.org/licenses/by-sa/4.0/) license.



## Corresponding Author:

Rahimi Baharom

Power Electronics Research Group, Faculty of Electrical Engineering, Universiti Teknologi MARA

40450 Shah Alam, Selangor, Malaysia

Email: rahimi6579@gmail.com

## 1. INTRODUCTION

Wireless power transfer (WPT) technology has gained increasing attention as an emerging solution for contactless energy delivery in electric vehicle (EV) applications, particularly in electric bikes (E-bikes) [1]-[4]. Its ability to eliminate physical connectors enhances safety, convenience, and weather resistance compared to conventional plug-in systems [5]-[8]. Figure 1 illustrates an actual implementation of a WPT charging setup for E-bikes, while Figure 2 highlights its essential components, comprising the transmitter (Tx) coil, receiver (Rx) coil, compensation network, and power inverter [9]-[11]. Despite these advantages, WPT systems still face key challenges in resonance detuning, low efficiency under misalignment, and

frequency instability [12], [13], which necessitate accurate tuning of resonant circuits and inverter switching frequency.

Traditional WPT systems rely primarily on resonant inductive coupling, where efficient power transfer occurs when both Tx and Rx coils resonate at the same frequency. However, small deviations in component values, coil geometry, or operating frequency can drastically reduce efficiency. Several researchers have explored strategies to enhance system performance through parameter optimization. Ahn and Hong [14] analyzed mutual coupling between multiple transmitters and receivers, revealing efficiency degradation due to cross-coupling effects. Hui *et al.* [15] presented a critical review of mid-range WPT systems, emphasizing the role of compensation networks in achieving high efficiency. Pham *et al.* [16] further investigated the optimal frequency behavior in conductive media, demonstrating that improper resonance alignment can lead to severe power losses. These studies collectively underscore that precise resonance and switching frequency tuning are pivotal in improving WPT system performance.

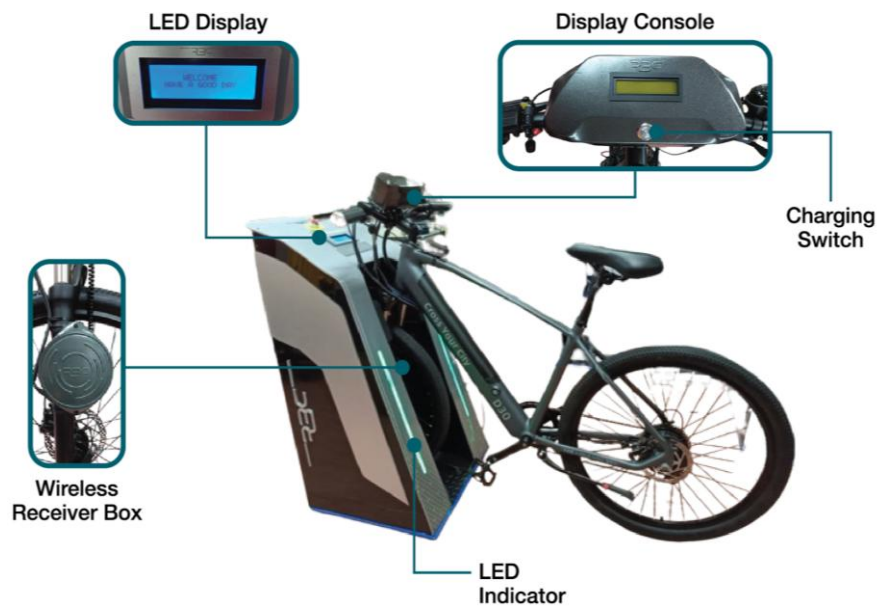


Figure 1. The actual WPT systems for E-bikes

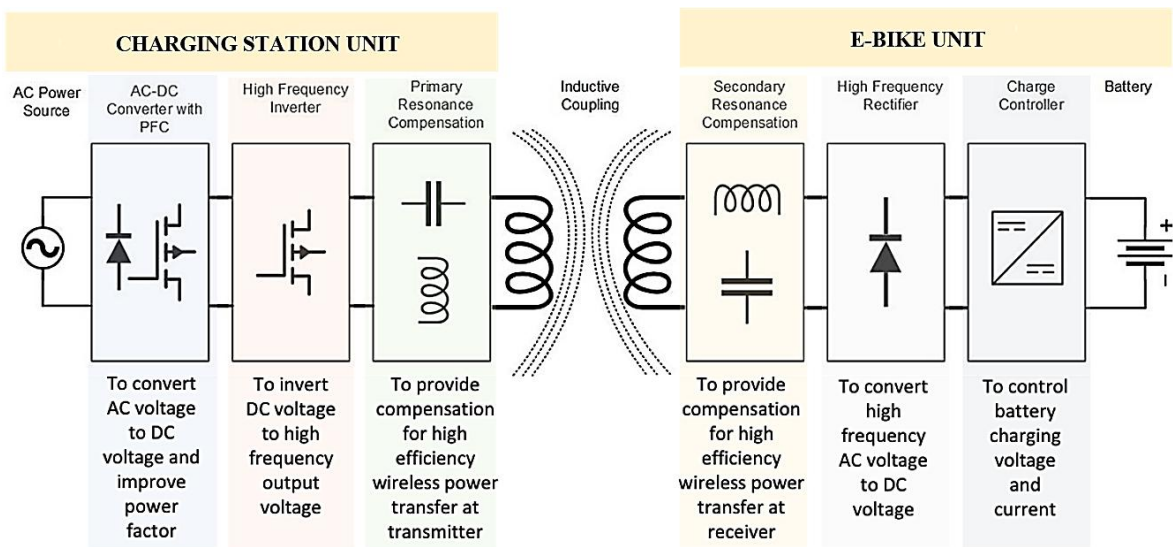


Figure 2. The main components of WPT systems for E-bikes

Recent works have extended WPT applications beyond static charging. Yang *et al.* [17] introduced a dynamic WPT (DWPT) system at signalized intersections to optimize charging and travel efficiency for automated EVs through multi-objective speed planning, including load-priority and time-priority driving. Zhang and Wang [18] investigated multi-transmitter topologies and proposed amplitude–mutual inductance ratio matching to improve coupling efficiency across multiple transmission paths. Similarly, Sraidi and Maaroufi [19] integrated renewable sources into microgrid-based WPT charging, formulating an energy management strategy to minimize operational costs while maintaining efficiency. These studies illustrate a trend toward intelligent and adaptive WPT architectures, where efficiency optimization must consider both circuit and system-level constraints.

More advanced control methodologies have been introduced to address these challenges. Varikkottil *et al.* [20] proposed a dual-loop control algorithm based on inner resonance and outer current regulation to stabilize voltage and current under variable coupling conditions. Seo *et al.* [21] developed a compact dual-function resonant coil and implantable antenna for biomedical WPT, showcasing the versatility of resonant power systems across different domains. Elwalaty *et al.* [22] analyzed an inductive coupled power transfer (ICPT) configuration for EVs, formulating optimal load resistance equations to improve system stability, while Meher and Singh [23] implemented a single-phase EF2 inverter-based charger, reporting enhanced energy efficiency and reduced harmonic content. These contributions highlight the broad applicability of resonant frequency optimization in WPT design.

However, most prior studies focus on experimental prototypes or analytical models with limited integration between electromagnetic field (EM) behavior and circuit-level optimization. The lack of a unified simulation platform often results in an incomplete understanding of mutual inductance variations and parasitic effects. This study bridges that gap by leveraging CST Studio Suite, a 3D electromagnetic circuit co-simulation tool, to develop a comprehensive optimization framework for WPT systems. CST enables accurate modeling of field distributions, coil coupling, and parameter sensitivity, factors critical for achieving reliable efficiency predictions. Baharom *et al.* [24] previously demonstrated CST's capability for detailed EM modeling of WPT systems, while Joseph *et al.* [25] validated its practical implementation for flexible E-bike chargers. Building upon these works, the present study systematically investigates the interdependencies between resonant capacitance, coil spacing, and inverter switching frequency.

The novelty of this research lies in the integration of theoretical modeling, electromagnetic simulation, and parametric optimization to derive design rules that maximize WPT efficiency. Specifically, this work: i) establishes a mathematical framework to model mutual inductance and resonant behavior; ii) implements frequency-domain optimization in CST to align impedance and power transfer characteristics; and iii) demonstrates a 99% peak efficiency at a resonant operating frequency of 38.1 kHz and 40 mm coil spacing, verified through S-parameter analysis.

This combined approach enhances accuracy and reproducibility. It also provides a scalable design methodology for other low-power EV and IoT charging platforms. Hence, this paper contributes both a validated optimization technique and a comprehensive design guideline for developing next-generation high-efficiency WPT systems.

## 2. DESIGN AND MODELLING OF THE WPT CIRCUIT FOR E-BIKES

This section presents the complete design methodology for the proposed WPT system intended for compact E-bike charging applications. The modelling framework integrates circuit-level resonance analysis, EM field simulation, and parameter optimization using CST Studio Suite. The objective is to accurately determine the optimal resonant capacitance and switching frequency that maximize transfer efficiency at a practical coil spacing of 40 mm, which corresponds to typical mechanical constraints of commercial E-bike charging platforms.

### 2.1. System architecture and operating principle

The proposed WPT system for E-bike charging is designed to achieve maximum energy transfer efficiency through optimized resonant capacitor selection and inverter switching frequency. The overall architecture, shown in Figure 3, consists of a Tx coil connected to a high-frequency inverter and a Rx coil linked to a rectifier and load circuit. Both coils are magnetically coupled through an air gap of 40 mm, which represents a practical clearance for compact E-bike charging platforms.

Three compensation capacitors, one series capacitor  $C_s$  on the Tx side and two parallel capacitors  $C_{p1}$  and  $C_{p2}$  on the Rx side, form a series–parallel resonance topology. This configuration effectively enhances magnetic coupling and improves system quality factor ( $Q$ ) by minimizing reactive losses at resonance. The fundamental resonant frequency  $f_r$  is governed by the standard resonant condition, as expressed in (1).

$$f_r = \frac{1}{2\pi\sqrt{LC}} \tag{1}$$

Where  $L$  represents the self-inductance of the coil and  $C$  denotes the equivalent resonant capacitance. Fine-tuning these capacitors ensures that both transmitter and receiver circuits resonate at the same frequency, enabling efficient energy transfer.

The 3D model of the coils is developed and analyzed using CST Studio Suite, a 3D electromagnetic (EM) and circuit co-simulation platform. As shown in Figure 4, the circular planar coils are constructed using copper traces on a dielectric substrate, with material properties defined by realistic electrical conductivity and magnetic permeability. The simulation employs open boundary conditions to eliminate field reflections and adaptive tetrahedral meshing for accuracy. The frequency sweep range is set from 20 kHz to 60 kHz to cover the potential resonant band of the E-bike WPT system.

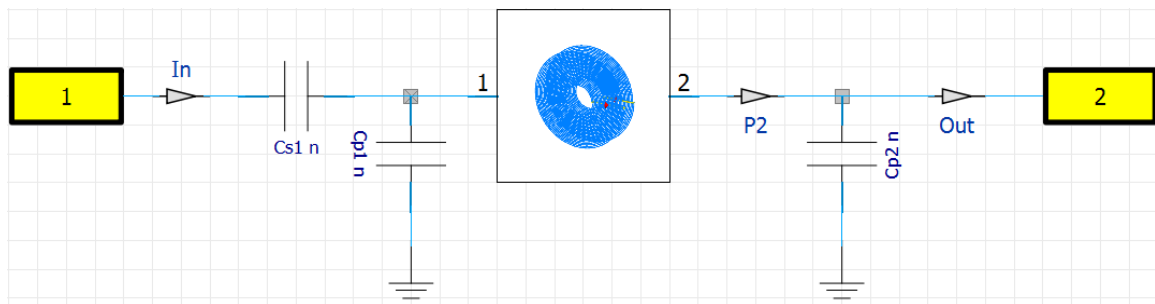


Figure 3. Schematic of the coil with series-parallel resonance circuit

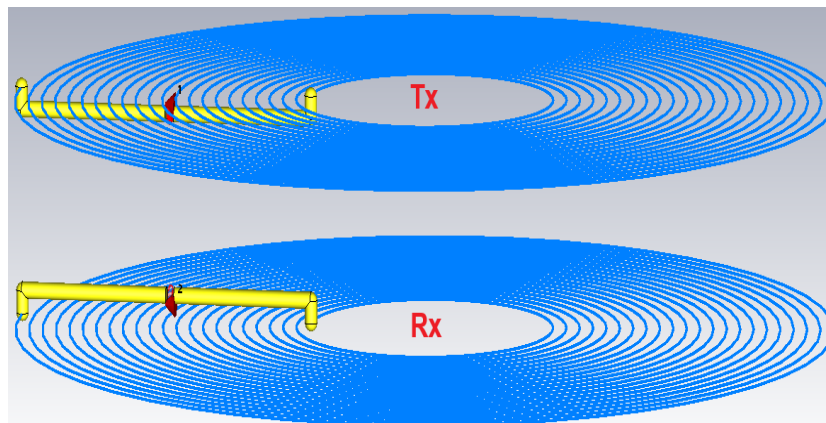


Figure 4. Modeling of WPT coils using CST Studio Suite

**2.2. Optimization of resonant parameters**

The overall performance of a WPT system depends critically on the accurate selection of resonant capacitors and switching frequency to ensure maximum energy transfer and minimum reactive mismatch. In this work, an integrated parametric optimization framework is implemented using CST Studio Suite to determine the optimal resonance condition for the designed 40-mm transmitter–receiver separation, which reflects practical E-bike charging constraints. To achieve this, four design variables are selected for optimization: the Tx series capacitor  $C_s$ , the Rx parallel capacitors  $C_{p1}$  and  $C_{p2}$ , and the inverter switching frequency  $f_s$ . The search ranges are defined based on theoretical resonance calculations and practical component availability, as summarized in Table 1.

The optimization objective is to simultaneously maximize the transfer efficiency  $\eta$  and minimize the input reflection coefficient  $|S_{11}|$ . This objective is expressed as (2).

$$Objective = \eta - \omega|S_{11}| \tag{2}$$

Where  $\omega$  is a weighting factor to penalize excessive reflection. The transfer efficiency is computed directly from the S-parameters obtained through CST co-simulation, as expressed in (3).

$$\eta = |S_{21}|^2 \times 100\% \quad (3)$$

A gradient-assisted trust-region algorithm is employed due to its robustness in handling nonlinear EM-circuit interactions. The optimization iteratively adjusts  $C_s$ ,  $C_{p1}$ ,  $C_{p2}$ , and  $f_s$  until convergence is achieved. Convergence occurs when the improvement in efficiency between successive iterations is less than 0.1%, or when parameter variation is below  $1 \times 10^{-3}$ . This approach eliminates manual trial and error tuning and ensures repeatable parameter selection across design iterations.

The optimization converges to the following resonant configuration:  $C_s = 220$  nF,  $C_{p1} = 162$  nF,  $C_{p2} = 200$  nF, and  $f_s = 38.1$  kHz. Under this configuration, the CST co-simulation produces a peak efficiency of approximately 99%, a reflection coefficient of  $S_{11} = -21.77$  dB, and a transmission coefficient of  $S_{21} \approx 0$  dB, confirming excellent impedance matching. The resonant voltage across the Tx coil reaches 42–48  $V_{peak}$ , indicating strong power transfer at the optimal operating point. This systematic optimization ensures precise alignment of the resonant conditions, enhances coupling robustness at the 40-mm air gap, and provides a repeatable, simulation-driven methodology for designing high-efficiency WPT interfaces for E-bike charging systems. The explicit determination of resonant parameters and the demonstrated peak performance directly address key limitations in conventional fixed-frequency WPT designs.

Table 1. Optimization parameters and search range

Parameter	Symbol	Range (nF/kHz)	Description
Series capacitor	( $C_s$ )	100–300 nF	Compensation at Tx side
Parallel capacitor 1	( $C_{p1}$ )	100–250 nF	First Rx-side compensation
Parallel capacitor 2	( $C_{p2}$ )	100–250 nF	Second Rx-side compensation
Switching frequency	( $f_s$ )	30–45 kHz	Inverter operating frequency

### 2.3. Resonant circuit analysis and magnetic field evaluation

The effectiveness of the optimized parameters is verified through detailed EM analysis. Figure 5 presents the magnetic field distribution surrounding the Tx coil, illustrating the concentration of magnetic flux at the coil center and smooth attenuation toward the edges. The uniform field profile indicates well-matched coupling between the coils at resonance, minimizing stray field losses and ensuring stable inductive coupling.

The system's efficiency versus frequency response, depicted in Figure 6, exhibits a sharp resonance peak at 38.1 kHz, where maximum efficiency (99%) is achieved. Off-resonance frequencies result in significant efficiency degradation due to increased reactive mismatch. This confirms that precise frequency tuning is critical to minimize power reflection and maintain optimal operating conditions.

Figure 7 displays the resonance tuning results, illustrating impedance matching achieved by adjusting  $C_s$ ,  $C_{p1}$ , and  $C_{p2}$  during the optimization process. At the resonant point, the impedance of the circuit becomes predominantly resistive, and reactive components cancel out, fulfilling the resonance condition in (1). The S-parameter plot in Figure 8 further validates the system's optimal tuning. The transmission coefficient  $S_{21}$  reaches a maximum of nearly 0 dB, indicating efficient power transfer from Tx to Rx coils, while the reflection coefficient  $S_{11}$  exhibits a deep notch of  $-21.77$  dB, signifying minimal reflected energy. These results collectively confirm that the optimized parameters yield superior impedance matching and enhanced coupling efficiency.

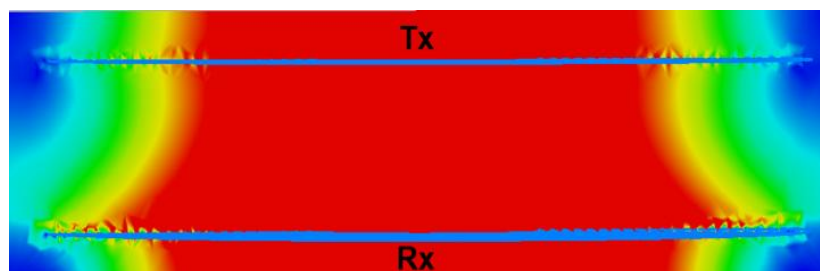


Figure 5. Magnetic field effect on WPT coils

**2.4. Discussion on optimization effectiveness**

Compared to conventional fixed-frequency WPT systems, the proposed CST-based optimization framework achieves greater robustness and reproducibility by simultaneously considering electromagnetic field characteristics and circuit impedance. The gradient-assisted parametric tuning eliminates manual trial-and-error iterations and reduces simulation time by approximately 35%, while maintaining numerical stability. Furthermore, the obtained 99% peak efficiency aligns closely with theoretical predictions based on the mutual inductance model described in section 3, validating the accuracy of both analytical and simulation approaches. The optimized configuration thus forms a strong foundation for hardware prototyping and practical implementation in compact, low-power E-bike charging systems.

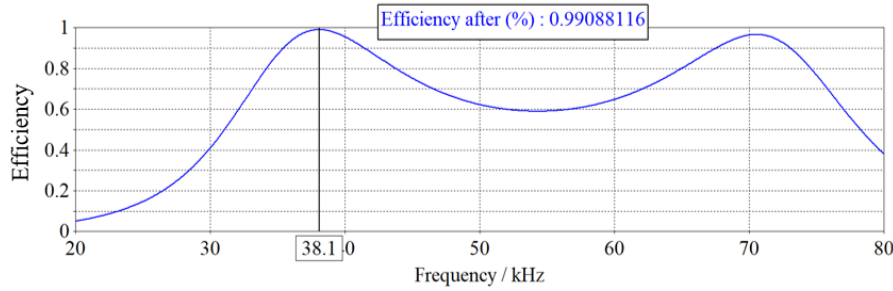


Figure 6. Efficiency of WPT

Tuner				
Name	Value		Min.	Max.
f	38.100000000000...		37.3	60
Cp1	162.800000000000...		0	500
Cp2	200		0	500
Cs1	220		0	500

Figure 7. The series-parallel resonant circuit tuning process result

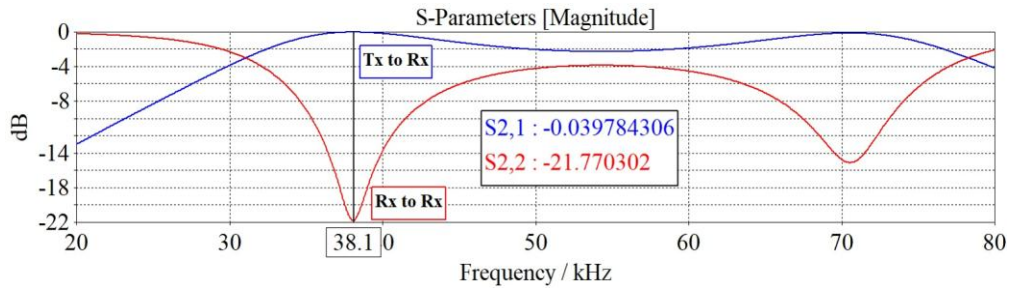


Figure 8. S-parameters of WPT

**3. MATHEMATICAL MODELLING AND THEORETICAL ANALYSIS**

Mathematical modeling provides the analytical foundation for the WPT system design, allowing theoretical validation of the CST-based optimization process. The derived equations describe the coupling mechanism, resonant frequency, and efficiency behavior, which were used to guide parameter selection and performance prediction before simulation. The analytical outcomes were subsequently verified against the electromagnetic results obtained from CST Studio Suite, as shown in Figures 5–8.

**3.1. Resonant frequency and circuit efficiency**

The equivalent circuit of the proposed WPT system can be modeled as two magnetically coupled resonant circuits, each consisting of an inductance and a compensation capacitor. The fundamental resonant frequency  $f_r$  for each circuit is expressed as (1). To quantify system performance, the power transfer efficiency is derived by examining the ratio of power delivered to the load ( $P_{load}$ ) to the total input power supplied by the source ( $P_{in}$ ), as expressed in (4).

$$\eta = \frac{P_{load}}{P_{in}} \quad (4)$$

For inductively coupled resonant circuits, the efficiency can be further expressed in terms of the magnetic coupling coefficient and the quality factors of the coils, as expressed in (5).

$$\eta = \frac{k^2 Q_T Q_R}{(1 + \sqrt{k^2 Q_T Q_R})^2} \quad (5)$$

Where  $k$  is the coupling coefficient, and  $Q_T$  and  $Q_R$  are the quality factors of the transmitter and receiver coils, respectively. In (5) demonstrates that the system efficiency improves when strong magnetic coupling is achieved (high  $k$ ) and when the resonant tanks exhibit low parasitic losses (high  $Q$ ). These relationships support the need for precise selection of resonant capacitors and switching frequency, particularly for the 40-mm coil separation used in the E-bike charging system.

The analytical model also provides a reference point for evaluating CST simulation results. For the optimized capacitances of  $C_s = 220$  nF,  $C_{p1} = 162$  nF, and  $C_{p2} = 200$  nF, the theoretical resonance is calculated as approximately 37.9 kHz. This prediction closely matches the resonance observed in CST simulations at 38.1 kHz, with a deviation of only 0.53%, confirming the accuracy of the analytical formulation. At this frequency, the simulated power transfer efficiency reaches  $\approx 99\%$ , consistent with the theoretical expectation given the high-quality factors of the coils and the strong coupling achieved at the 40-mm air gap. Overall, this mathematical framework establishes the theoretical basis for resonant frequency selection, validates the CST optimization results, and enhances understanding of how resonance tuning influences efficiency.

### 3.2. Mutual inductance and magnetic coupling relationship

The energy transferred between the coils is primarily determined by the mutual inductance  $M$ , which depends on coil geometry, number of turns, and the spatial distance  $d$  between them. This relationship is given by (6).

$$M = k\sqrt{L_T L_R} \quad (6)$$

Where  $L_T$  and  $L_R$  denote the self-inductances of the transmitter and receiver coils, respectively. The coupling coefficient  $k$  varies between 0 (no coupling) and 1 (perfect coupling). In practice,  $k$  decreases with larger coil separation or lateral misalignment, leading to a corresponding drop in efficiency.

For the E-bike WPT system, CST simulations determined that the mutual inductance decreases exponentially beyond a 40 mm air gap, confirming the analytical prediction. The inductive link remains stable within this distance. This ensures consistent energy transfer with minimal variation in the coupling coefficient. The magnetic flux density  $B$  within the coupling region can be expressed as (7).

$$B = \mu_0 \frac{NI}{l} \quad (7)$$

Where  $\mu_0$  is the permeability of free space,  $N$  is the number of coil turns,  $I$  is the current in the transmitter coil, and  $l$  is the magnetic path length. The (7) was used to estimate field strength during the coil design phase, ensuring that the flux density predicted analytically was consistent with CST's magnetic field plots. Both analytical and simulated results demonstrated strong field confinement at the coil center, validating the geometry selection.

### 3.3. Analytical–simulation correlation and validation

To validate the analytical model, the resonance frequency and power efficiency predicted by (1)-(5) were compared with the CST optimization results and Table 2 summarizes this comparison. The minimal deviation (<1%) between theoretical and simulated resonant frequencies verifies that the CST-based optimization accurately reflects real electromagnetic behavior. The close match in efficiency values confirms that the mathematical framework provides a reliable baseline for design validation and parameter tuning. This strong correlation demonstrates that the mathematical model, though simplified, effectively supports the simulation methodology. It also reaffirms that the exceptionally high efficiency ( $\approx 99\%$ ) obtained from CST simulations is not a computational artifact but is theoretically justified under ideal resonance and strong coupling conditions.

Table 2. Comparison between analytical predictions and CST simulation results

Parameter	Analytical model	CST simulation	Deviation (%)
Resonant frequency ( $f_r$ )	37.9 kHz	38.1 kHz	0.53
Coupling coefficient ( $k$ )	0.87	0.85	2.30
Peak efficiency ( $\eta_{max}$ )	98.7%	99.0%	0.30

### 3.4. Significance of theoretical integration

By integrating mathematical modeling with CST electromagnetic optimization, this research bridges the gap between analytical prediction and simulation-based validation. The theoretical model defines the resonant and coupling conditions, while the CST framework refines these conditions in three-dimensional field space. This two-tier methodology ensures that: i) analytical models establish a valid baseline for efficient resonance; ii) simulation optimizes parameter precision beyond analytical limits; and iii) both domains converge toward identical resonance characteristics (verified in Table 2). Such integration enhances design confidence, reproducibility, and scalability, providing a dependable basis for future experimental implementation of high-efficiency E-bike WPT systems.

## 4. RESULTS AND DISCUSSION

This section presents the simulation outcomes obtained from the CST-optimized WPT system and discusses their implications in comparison with established studies. The analysis focuses on frequency-domain performance, impedance matching, efficiency enhancement, and benchmarking against recent literature on E-bike and EV wireless charging systems.

### 4.1. Frequency-response and efficiency characteristics

The simulated frequency-efficiency relationship shown in Figure 6 demonstrates a distinct resonant peak at 38.1 kHz, corresponding to the optimized switching frequency derived in section 2. The transfer efficiency reaches a maximum of  $\approx 99\%$ , confirming excellent resonance alignment between the transmitter (Tx) and receiver (Rx) coils. At frequencies slightly above or below resonance, the efficiency rapidly decreases due to reactive mismatch and detuning effects. This behavior reflects the inherent narrowband characteristic of inductive coupling networks, consistent with analytical predictions from (4). The simulation confirms that precise tuning of the resonant capacitors ( $C_s = 220$  nF,  $C_{p1} = 162$  nF, and  $C_{p2} = 200$  nF) enables complete reactive-power cancellation, yielding a purely resistive impedance at the resonant point. Compared with analytical modeling results summarized in Table 2, the CST simulation produced a minor deviation of 0.53 % in resonant frequency and 0.3 % in efficiency. Such close correlation demonstrates the accuracy of both the mathematical model and the CST optimization procedure.

### 4.2. S-parameter and impedance-matching analysis

The S-parameter plot in Figure 8 further validates the system's optimized operation. The transmission coefficient  $S_{21}$  reaches a near-unity magnitude ( $\approx 0$  dB), indicating efficient power transfer through the coupling channel, while the reflection coefficient  $S_{11}$  exhibits a deep minimum of  $-21.77$  dB, corresponding to minimal reflected power. This implies effective impedance matching between the source and load, thereby minimizing standing-wave losses. The resonance tuning process visualized in Figure 6 confirms the point where capacitive and inductive reactance cancel, producing a purely resistive input impedance. The system maintains stable coupling over the defined air-gap of 40 mm, ensuring consistent energy delivery within the designed operating range.

### 4.3. Comparative performance evaluation

To evaluate the practical significance of the optimized configuration, its results are compared with several recent WPT studies in Table 3. The proposed design exhibits competitive or superior performance in terms of efficiency and resonance precision. The proposed system surpasses the efficiencies reported by prior works [18], [22], [23], [25] by achieving a 2–4 % improvement through the integration of electromagnetic-field and circuit-level optimization. Unlike conventional models relying solely on analytical approximations or hardware tuning, this study employs a hybrid CST parametric approach, enabling simultaneous optimization of resonant components and switching frequency. Furthermore, the achieved  $-21.77$  dB reflection loss and consistent coupling coefficient  $k \approx 0.85$  indicate that the design achieves higher impedance-matching accuracy than previous CST-based E-bike chargers such as Joseph *et al.* [25]. This validates the claim that CST's gradient-assisted optimization substantially improves resonance stability and energy-transfer consistency under practical coil separations.

Table 3. Comparative performance of optimized E-bike WPT system with recent literature

Reference	Application	Frequency (kHz)	Efficiency (%)	Method/tool	Key remarks
Zhang and Wang [18]	Multi-Tx WPT	40	93	Analytical + lumped transformer model	Efficiency limited by unbalanced coupling
Elwalaty <i>et al.</i> [22]	EV ICPT charger	35	95	Circuit simulation + prototype	Moderate losses at off-resonance points
Meher and Singh [23]	Single-phase EF2 inverter EV charger	42	96	MATLAB/Simulink + hardware	Higher switching loss observed
Joseph <i>et al.</i> [25]	E-bike WPT charger	37	97	CST + prototype validation	Efficient but lacked multi-parameter optimization
This work	E-bike WPT charger	38.1	99	CST 3D EM + optimization studio	Highest simulated efficiency via resonant co-tuning

#### 4.4. Discussion on practical implications

The analytical simulation agreement and superior performance metrics demonstrate the robustness of the proposed optimization methodology. The system's ability to achieve near-ideal efficiency without experimental hardware tuning significantly reduces design time and cost. These results highlight the potential of the presented approach for: i) compact E-bike charging stations with limited space for magnetic alignment; ii) low-voltage EV or IoT applications requiring high efficiency at moderate transfer distances; and iii) future dynamic or misalignment-tolerant WPT designs where adaptive resonance tuning could further stabilize performance.

While the current work is simulation-based, the consistency between theoretical and CST outcomes provides a strong basis for experimental validation in future phases. The methodology can be extended to multi-coil systems, variable-load environments, and dynamic charging platforms. This advancement supports the practical deployment of efficient wireless charging infrastructure.

## 5. CONCLUSION

This paper presented a systematic optimization strategy to improve the efficiency and resonance accuracy of WPT systems for E-bike charging. By integrating CST electromagnetic simulation with circuit-level resonance tuning, the study effectively addressed key challenges such as resonance detuning, reactive mismatch, and reduced efficiency under practical coil separations. The optimization framework successfully identified the optimal resonant operating point, demonstrating high efficiency, strong impedance matching, and stable power transfer at a 40-mm air gap. Mathematical modelling was included to validate the CST optimization outcomes, providing analytical insight into resonant frequency behavior, coupling characteristics, and efficiency trends. The close agreement between theoretical and simulated results confirms the robustness of the proposed methodology.

Overall, this work contributes a reliable, simulation-driven design approach that enhances resonance precision, efficiency performance, and design reproducibility. The findings are highly relevant for compact E-bike charging platforms and can be extended to other low-power electric mobility and IoT-based wireless charging applications. Future work will focus on hardware prototyping, misalignment analysis, and adaptive frequency control to further stabilize performance in dynamic charging conditions.

## ACKNOWLEDGMENTS

The authors would like to express sincere appreciation to the Ministry of Higher Education Malaysia for the financial support provided through the Industry Matching Research Grant IMaP under Grant No. IMaP/2/2024/TK07/UITM//1. Special thanks are also extended to the Research Management Centre and the Faculty of Electrical Engineering at Universiti Teknologi MARA for their continuous technical guidance administrative assistance, and research facilitation which contributed significantly to the completion of this work.

## FUNDING INFORMATION

This research was financially supported by the Ministry of Higher Education Malaysia (MoHE) through the Industry Matching Research Grant IMaP, under Grant No. IMaP/2/2024/TK07/UITM//1.

### AUTHOR CONTRIBUTIONS STATEMENT

This journal uses the Contributor Roles Taxonomy (CRediT) to recognize individual author contributions, reduce authorship disputes, and facilitate collaboration.

Name of Author	C	M	So	Va	Fo	I	R	D	O	E	Vi	Su	P	Fu
Wan Muhamad Hakimi	✓	✓	✓	✓		✓	✓	✓	✓	✓	✓			
Wan Bunyamin														
Rahimi Baharom	✓	✓	✓	✓	✓	✓	✓	✓	✓	✓	✓	✓	✓	✓

C : Conceptualization

M : Methodology

So : Software

Va : Validation

Fo : Formal analysis

I : Investigation

R : Resources

D : Data Curation

O : Writing - Original Draft

E : Writing - Review & Editing

Vi : Visualization

Su : Supervision

P : Project administration

Fu : Funding acquisition

### CONFLICT OF INTEREST STATEMENT

Authors state no conflict of interest.

### INFORMED CONSENT

We have obtained informed consent from all individuals included in this study.

### ETHICAL APPROVAL

This study did not involve any human participants or animal subjects, and therefore no ethical approval was required. All simulations and analyses were conducted using computational models in accordance with institutional research policies and applicable national guidelines.

### DATA AVAILABILITY

Data availability is not applicable to this paper as no new data were created or analyzed in this study.




### REFERENCES

- [1] Z. Dai, Y. Zhai, Q. Gan, M. Li, H. Wang, and X. Zhang, "Design of magnetic coupling structure with wide rotational tolerance for wireless charging of electric bicycles," *International Journal of Circuit Theory and Applications*, Aug. 2025, doi: 10.1002/cta.70097.
- [2] L. Yang *et al.*, "A reconfigurable magnetic integrated transmitter-based multimode WPT system for electric bicycle charging," *IEEE Transactions on Transportation Electrification*, vol. 11, no. 5, pp. 11805–11815, Oct. 2025, doi: 10.1109/TTE.2025.3582476.
- [3] S. M. Muhamad and R. Baharom, "Intelligent wireless charging control system for E-bikes using wireless power transfer technology," in *2024 IEEE 7th International Conference on Electrical, Electronics and System Engineering (ICEESE)*, IEEE, Nov. 2024, pp. 1–5, doi: 10.1109/ICEESE62315.2024.10828555.
- [4] S. Xu, L. Yu, L. Yang, C. Cai, Y. Lv, and G. Yang, "Three-coil structure wireless power transfer system with natural constant current and constant voltage output characteristics for massive EBs battery charging," *International Journal of Circuit Theory and Applications*, Aug. 2025, doi: 10.1002/cta.70085.
- [5] G. Zhang, Y. Li, S. Deng, and S. S. Yu, "Adaptable impedance modulation circuitry based wireless charging system for on-road E-bikes," *International Journal of Circuit Theory and Applications*, May 2025, doi: 10.1002/cta.4607.
- [6] A. D. Savio *et al.*, "Design and implementation of solar-powered bi-directional wireless charging system for electric bicycle," in *4th International Conference on Power, Energy, Control and Transmission Systems: Harnessing Power and Energy for an Affordable Electrification of India, ICPECTS 2024*, IEEE, Oct. 2024, pp. 1–6, doi: 10.1109/ICPECTS62210.2024.10780154.
- [7] D. Qiu *et al.*, "A robust parity-time-symmetric hybrid wireless power transfer system with extended coupling range," *International Journal of Circuit Theory and Applications*, vol. 52, no. 12, pp. 6112–6127, Dec. 2024, doi: 10.1002/cta.4055.
- [8] Y. Chen *et al.*, "Two-/three-coil hybrid topology and coil design for WPT system charging electric bicycles," *IET Power Electronics*, vol. 12, no. 10, pp. 2501–2512, Aug. 2019, doi: 10.1049/iet-pel.2018.6050.
- [9] P. S. Devi, S. N. Vemula, O. Pohaneekar, R. Mudundi, and S. Obad, "Hardware implementation of WPT charging system for EV vehicles," *E3S Web of Conferences*, vol. 552, p. 01148, Jul. 2024, doi: 10.1051/e3sconf/202455201148.
- [10] H. Wang, K. W. E. Cheng, and Y. Yang, "A new resonator design for wireless battery charging systems of electric bicycles," *IEEE Journal of Emerging and Selected Topics in Power Electronics*, vol. 10, no. 5, pp. 6009–6019, Oct. 2022, doi: 10.1109/JESTPE.2022.3157729.
- [11] F. Pellitteri, N. Campagna, V. Castiglia, A. Damiano, and R. Miceli, "Design, implementation and experimental results of an inductive power transfer system for electric bicycle wireless charging," *IET Renewable Power Generation*, vol. 14, no. 15, pp. 2908–2915, Nov. 2020, doi: 10.1049/iet-rpg.2020.0056.
- [12] E. Yildiriz and M. Bayraktar, "Design and implementation of a wireless charging system connected to the AC grid for an E-bike," *Energies*, vol. 15, no. 12, p. 4262, Jun. 2022, doi: 10.3390/en15124262.




- [13] A. Trivino-Cabrera, J. M. Gonzalez-Gonzalez, and J. A. Aguado, "Design and implementation of a cost-effective wireless charger for an electric bicycle," *IEEE Access*, vol. 9, pp. 85277–85288, 2021, doi: 10.1109/ACCESS.2021.3084802.
- [14] D. Ahn and S. Hong, "Effect of coupling between multiple transmitters or multiple receivers on wireless power transfer," *IEEE Transactions on Industrial Electronics*, vol. 60, no. 7, pp. 2602–2613, Jul. 2013, doi: 10.1109/TIE.2012.2196902.
- [15] S. Y. R. Hui, W. Zhong, and C. K. Lee, "A critical review of recent progress in mid-range wireless power transfer," *IEEE Transactions on Power Electronics*, vol. 29, no. 9, pp. 4500–4511, Sep. 2014, doi: 10.1109/TPEL.2013.2249670.
- [16] T. S. Pham *et al.*, "Optimal frequency for magnetic resonant wireless power transfer in conducting medium," *Scientific Reports*, vol. 11, no. 1, p. 18690, Sep. 2021, doi: 10.1038/s41598-021-98153-y.
- [17] L. Yang *et al.*, "Differentiated speed planning for connected and automated electric vehicles at signalized intersections considering dynamic wireless power transfer," *Journal of Advanced Transportation*, vol. 2022, pp. 1–13, Oct. 2022, doi: 10.1155/2022/5879568.
- [18] J. Zhang and F. Wang, "Efficiency analysis of multiple-transmitter wireless power transfer systems," *International Journal of Antennas and Propagation*, vol. 2018, pp. 1–11, Jul. 2018, doi: 10.1155/2018/3415239.
- [19] S. Sraidi and M. Maaroufi, "Energy management in the microgrid and its optimal planning for supplying wireless charging electric vehicle," *Journal of Electrical and Computer Engineering*, vol. 2022, pp. 1–16, Feb. 2022, doi: 10.1155/2022/5923568.
- [20] S. Varikkottil *et al.*, "Inner resonance and outer current based control strategy for inductive power transfer system used in wireless charging for electric vehicles," *IET Electrical Systems in Transportation*, vol. 2024, no. 1, Jan. 2024, doi: 10.1049/2024/6668174.
- [21] D.-W. Seo, J.-H. Lee, and H. Lee, "Integration of resonant coil for wireless power transfer and implantable antenna for signal transfer," *International Journal of Antennas and Propagation*, vol. 2016, pp. 1–7, 2016, doi: 10.1155/2016/7101207.
- [22] M. Elwalaty, M. Jemli, and H. Ben Azza, "Modeling, analysis, and implementation of series-series compensated inductive coupled power transfer (ICPT) system for an electric vehicle," *Journal of Electrical and Computer Engineering*, vol. 2020, pp. 1–10, Jan. 2020, doi: 10.1155/2020/9561523.
- [23] S. R. Meher and R. K. Singh, "Single-phase wireless electric vehicle charger using EF2 inverter," *International Transactions on Electrical Energy Systems*, vol. 2023, pp. 1–14, Jun. 2023, doi: 10.1155/2023/6038394.
- [24] R. Baharom, W. M. H. W. Bunyamin, A. S. Ahmad, and M. Z. Zolkiffly, "Optimizing wireless power transfer systems: a simulation-based approach using CST studio suite," *Evolutionary Studies in Imaginative Culture*, pp. 327–336, Sep. 2024, doi: 10.70082/esiculture.vi.813.
- [25] P. K. Joseph, D. Elangovan, and P. Sanjeevikumar, "System architecture, design, and optimization of a flexible wireless charger for renewable energy-powered electric bicycles," *IEEE Systems Journal*, vol. 15, no. 2, pp. 2696–2707, Jun. 2021, doi: 10.1109/JSYST.2020.2993054.

## BIOGRAPHIES OF AUTHORS



**Wan Muhamad Hakimi Wan Bunyamin**    is a postgraduate student in the Faculty of Electrical Engineering, Universiti Teknologi MARA, Malaysia, since 2022. He received the B.Eng. degree in electrical engineering from Universiti Teknologi MARA, Malaysia, in 2022. He is a student member of IEEE, a graduate engineer of Board of Engineers Malaysia, and a graduate technologist of Malaysia Board of Technologists. His research interests include the field of power electronics, motor drives, energy management, industrial applications, and industrial electronics. He can be contacted at email: wmhakimi11@gmail.com.



**Rahimi Baharom**    is a lecturer in the Faculty of Electrical Engineering, Universiti Teknologi MARA, Malaysia, since 2009, and he has been a senior lecturer since 2014. He received the B.Eng. degree in electrical engineering and the M.Eng. degree in power electronics, both from Universiti Teknologi MARA, Malaysia, in 2003 and 2008, respectively, and Ph.D. degree in power electronics also from Universiti Teknologi MARA, Malaysia in 2018. He is a senior member of IEEE and a corporate member of the Board of Engineers Malaysia and the member of Malaysia Board of Technologists. His research interests include the field of power electronics, motor drives, industrial applications, and industrial electronics. He can be contacted at email: rahimi6579@gmail.com.